Infrared small target detection based on Gaussian curvature filtering and partial sum of singular values

Junchang Zhang*, Pu Liu, Jiaming Xie, Meiyu Li

School of Electronic Information, Northwestern Polytechnical University, Xi'an, Shaanxi, China

ABSTRACT

To reduce noise and background distractions, we propose a detection algorithm based of Gaussian curvature filtering (GCF) and partial sum of singular values (PSSV). Above all, aiming at the false alarms caused by noise, using the prior knowledge of natural image have the characteristics of approximate developable, GCF utilizes the variation model to obtain an approximately noise-free image. Secondly, we adopt PSSV to suppress the background by pointing out that the reason why Robust PCA is inaccurate in the background estimation is that the hypothesis at the edge of the background does not match the reality, and we present a model solving algorithm on the ground of imprecise augmented Lagrangian multiplier method (IALM). At last, we use an adaptive threshold segmentation algorithm to segment the target. The model has better noise clutter suppression and detection accuracy than other representative methods.

Keywords: Infrared image, Gaussian curvature, singular value partial sum, background estimation

1. INTRODUCTION

Infrared detection technology, as an indirect contact-type non-active detection related technology, has better concealment, stronger anti-interference ability and ability to work around the clock than visible light systems and radar[1]. The detection methods of infrared small target on the ground of single frame image mainly use the spatial information of single frame image to give a decision whether the target exists or not[2]. Existing infrared small target detection method on the ground of single frame image are mainly divided into three types[3].

Firstly, in target-based detection methods, the characteristics of the target are mainly used for target screening, such as grayscale, contrast, local difference, and gradient[4]. For example, the method on the ground of local contrast (Local Contrast method, LCM)[5] first calculates the enhancement factor, the rate of a local center and its neighborhood in the image, and then multiplies the local center value and the enhancement factor. This makes it easier to distinguish the target and background[6]. To improve the detection rate in complex scenes, Qin et al. proposed a novel local contrast measure (novel local contrast measure, NLCM)[7] method. Liu[8] et al. uses a gradient vector field, combining target's gradient and sink characteristics to complete the precise positioning of the target. In highly complex contexts, clutter is mixed with small and medium targets, which inevitably leads to a serious false alarm rate.

Secondly, the detection method based on background features mainly estimates the background signal of the image from the perspective of the spatial domain and the transform domain, and then use the initial image and the estimated background. Hadhoud et al. proposed the TDLMS method[9] on the ground of LMS (least mean square), from one dimension to two dimensions. The method first performs error function calculation on the template parameters according to the content of the input image, when the error function value is less than the threshold, stop the iteration and output the background image predicted by this method.

Thirdly, the detection method on the ground of image data structure uses the different structure characteristics such as the sparsity of the target and the low rank of the background[10]. Among them, the representative method is based on Infrared patch-image (IPI) model[11], recovering sparse matrix components and low-rank matrix components from the data matrix. However, for infrared small targets in complex environment, the target is mixed with strong clutter signals, which increases the false alarm rate[12].

In accordance with these problems, from the perspective of noise and clutter background, this paper takes the noise that

* zhangjc@nwpu.edu.cn

Third International Conference on Computer Science and Communication Technology (ICCSCT 2022)
edited by Yingfa Lu, Changbo Cheng, Proc. of SPIE Vol. 12506, 125063P
© 2022 SPIE · 0277-786X · doi: 10.1117/12.2662481

is very similar to the target in terms of gray scale and other features, and adopts the Gaussian curvature variational model to de-noising infrared images according to the prior conditions that natural images can be developed everywhere. Then, aiming at the defect of poor segmentation performance based on IPI model in complex background, the analysis concluded that the reason was the mismatch between the implicit assumption of IPI model for many observations and the insufficiency of strong edge observations. Therefore, the constraint of the singular value part of infrared block image and (IPPS) was used to repair the defect, and IALM was used to solve it.

2. GAUSSIAN CURVATURE FILTERING

Generally speaking, a single frame infrared image is modeled as:

$$f(x,y,t) = f_B(x,y,t) + f_T(x,y,t) + N(x,y,t) \tag{1}$$

where, $f_B(x,y,t)$ and $f_T(x,y,t)$ represent the gray value of background and target at point (x,y) respectively, and $N(x,y,t)$ refers to the gray value of noise.

It is a morbid problem to restore the real image from the discrete infrared noise image. Therefore, additional prior knowledge assumptions must be made on the real image. Our aim is to restore unknown estimates of potential perfect images from observed discrete samples. The reconstruction problem can be expressed in a variational form as:

$$\hat{U} = \arg\min_{U\in\Omega}\left\{ \int_{x\in\Omega} \Phi_0(U,I)dx + \lambda \int_{x\in\Omega} \Phi_1(U)dx \right\} \tag{2}$$

where Φ_0 is a data fitting cost function, which measures the approximate degree of the estimated infrared image and infrared observation image after transformation. Φ_1 constitutes a priori, namely the regularization function on U, scalar weighted coefficient λ is the regularization coefficient, which regulates the trade-off between fitting term and regularization, and Ω is the image domain space.

It is proved that it is as difficult to choose proper prior knowledge as to solve the original problem. Improper prior knowledge may blur the features in the image or lead to wrong results. Natural images have a good developable surface property, that is, the Gaussian curvature of natural images is approximately 0, as shown in Figure 1, and the existence of noise will weaken this property. The representation of Gaussian curvature is as follows:

$$K(U(x)) = \frac{U_{xx}U_{yy} - U_{xy}^2}{(1+U_x^2+U_y^2)^2} \tag{3}$$

where U_x and U_y are the first partial derivatives of the initial picture, U_{xx}, U_{xy} and U_{yy} are the second partial derivatives of the initial picture.

It can be seen from Figure 1 that Gaussian curvature is an ideal prior condition. As a prior knowledge, Gaussian curvature can better retain the edge part of the image, and the variational problem of the denoising model is changed into the following form:

$$\min_{U\in\Omega}\left\{ \varepsilon(U) = \int_\Psi |K(U)|\, d\Psi \right\}, \quad s.t. \quad \int_\Omega |U-I|^2\, dx < \varepsilon \tag{4}$$

where $\varepsilon(U)$ is gaussian curvature energy, and ε is a very small evolutionary termination threshold. from the Angle of differential geometry, this paper uses gaussian curvature property of the image to solve the variational model.

Based on the property that noiseless images are piecewise developable, there is the theorem that for any point on a developable surface, it lies on the section of a point in its neighborhood. For infrared images with noise, it is necessary to reduce the Gaussian curvature to achieve piecewise developable[13], so we need to use the image discreteness to strucure the section. In the small window of 3*3, all possible sections can be enumerated. By taking advantage of the discreteness of data, all possible sections can be traversed, and then the smallest change in the current gray value can be found for updating, which completes a Gaussian curvature filter.

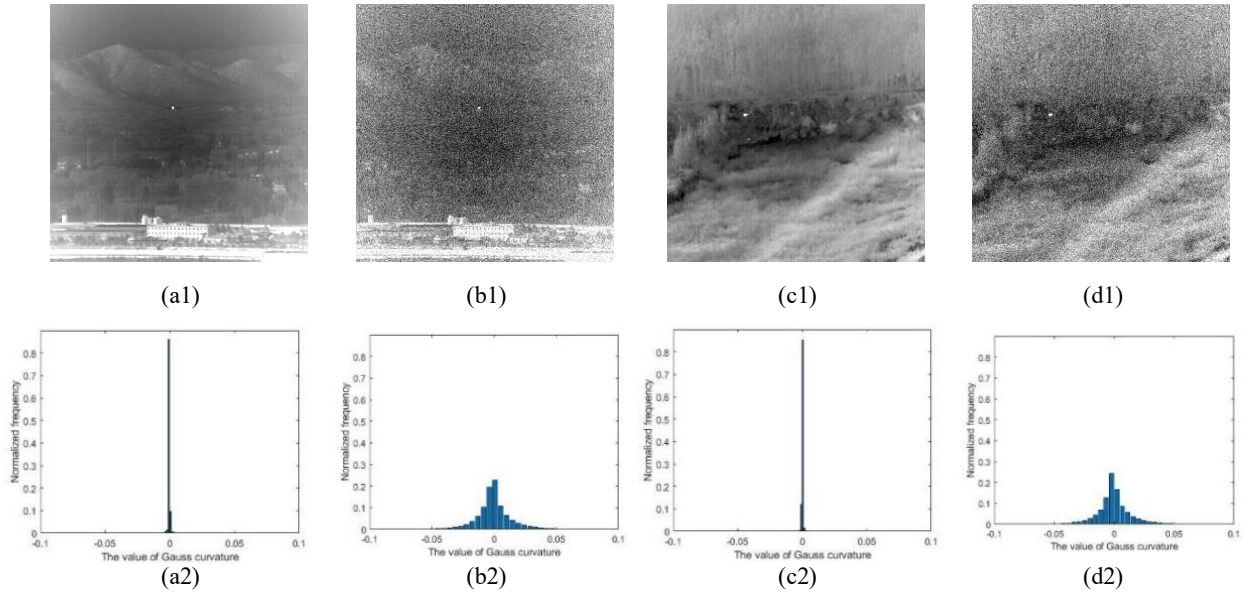

Figure 1. In Infrared image (top) and normalized frequency of Gaussian curvature (bottom). (a): Infrared image without noise under ground background; (b): infrared image with noise under ground background; (c): infrared image without noise under sea surface background; (d): infrared image with noise under sea surface background.

The updating process of Gaussian curvature filter can be divided into four stages: image domain decomposition, enumerating all tangent planes and projection distances, and finding the minimum projection operator. The whole pixel is divided into four parts, which can be represented by (black triangle), (white triangle), (white circle) and (black circle) respectively.

Based on any point on a developable surface is located in its neighborhood within a certain point on the plane of the prior conditions, in this article the tangent plane is based on eight areas, with a triangular configuration tangent plane projection operator is a total of 12, as shown in Figure 2, the black circle is a center pixel, white circle represents the adjacent pixels, and dotted line is the neighborhood of tangent plane[14]. In fact, there are only four types from the center point to the eight tangent planes. For example, the distance from the center BC to the two triangle tangent planes formed by two WT and one WC is the same, and so on, so there are a total of 8 effective tangent planes. The distance between the center pixel and the eight minimum triangular tangent planes $\{I_i, i=1,2,\ldots,9\}$ is calculated, the minimum projection distance $I_{\min}$ is selected to represent the distance between the current image $U(x)$ and the target image $U_1(x)$, and $U_1(x)=U(x)+I_{\min}$ is used to complete an update.

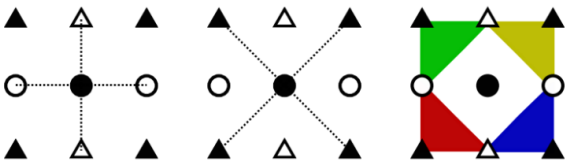

Figure 2. Tangent plane type.

3. IPPS MODEL

An infrared block image model (IPI) is presented by Gao C et al.[15], transforming the original image into an block image model. IPI divides the original infrared image into overlapping blocks with a sliding window and pull it into a column vector. The IPI-based method segments well for relatively simple and smooth background. However, for relatively

complex background, it is easy to mistake the edge of the thick cloud layer as a sparse part and segment it into the target block.

We think the background changes slowly. That is to say there is a high correlation between the divided images and the divided images. The traditional low-rank model hypothesizes that the background block comes from a low-rank subspace, and kernel norm is used to describe it, which is only suitable for describing background block images when there are a large number of samples. In a complex background, considering the unavoidable structure of defective examples, the partial sum of singular values is used to describe the background patch image, shown in the following formula:

$$\|B\|_{*,\le r} = \|B\|_{p=N} = \sum_{i=N+1}^{\min(m,n)} \sigma_i(B) \tag{5}$$

In the formula, σ_i is the i-th maximum singular value of background B, and r is the biggest limitation of the ratio of σ_N to σ_i. For infrared images, since the complexity of the background is unknown, we can not point out a fixed rank limitation. But at the same time, because the small target is only a small part, no matter how the background changes, we can install a fixed energy rate limitation. Given g, the retained rank can be easily calculated.

The object is only a small part of the image, so we consider the target sub-image as a sparse matrix, that is, the value of most elements is 0. In addition, the target is brighter than the surrounding area, that is, the real the value of the target is usually positive. Thus, an additional non-negative constraint should be introduced to the target patch image. So the overall constraint equation is explained as:

$$\min_{B,T} \|B\|_{*,\le r} + \lambda \|T\|_{1,\ge 0}, \qquad s.t.\ D = B + T, T \ge 0 \tag{6}$$

λ is a weight parameter, thus, the original detection becomes optimization, and its augmented Lagrangian function is expressed as:

$$L(B,T,Y,\mu) = \|B\|_{*,\le \gamma} + \lambda \|T\|_{1,\ge 0} + \left\langle Y^T, (D-B-T) \right\rangle + \frac{\mu}{2} \|D-B-T\|_F^2 \tag{7}$$

The linearized alternating direction method IALM with adaptive penalty is used to solve the problem.

$$\begin{aligned} B^{k+1} &= \arg\min\ L(B,T^k,Y^k,\mu_k) \\ &= \arg\min \mu_k^{-1} \|B\|_{*,\le \gamma} + \frac{1}{2} \|B - (D - T^k - Y^k / \mu_k)\|_F^2 \end{aligned} \tag{8}$$

$$\begin{aligned} T^{k+1} &= \arg\min\ L(B^{k+1},T^k,Y^k,\mu_k) \\ &= \arg\min \lambda\mu_k^{-1} \|T\|_{1,\ge 0} + \frac{1}{2} \|B - (D - B^{k+1} + Y^k / \mu_k)\|_F^2 \end{aligned} \tag{9}$$

We use the following Theorem 1 and Theorem 2 to solve the above problem. As followed, Algorithm 1 gives the solution process.

Theorem 1: Let $\tau > 0$ and $X, Y \in R^{m*n}$, transform non-negative l_1-norm minimisation into $\arg\min_X \frac{1}{2}\|X-Y\|_F^2 + \tau\|X\|_1$ can be solved by a non-negative soft threshold operator $S_{\tau\ge 0}(x) = \max(x-\tau, 0)$.

Theorem 2: Let $\tau > 0$, $l = \min(m,n)$ $X, Y \in R^{m*n}$, Y can be written as $Y = Y_1 + Y_2 = U_{Y_1} S_{Y_1} V_{Y_1}^T + U_{Y_2} S_{Y_2} V_{Y_2}^T$, where U_{Y_1} and V_{Y_1} are the singular vector matrices in keeping with the *n-th* maximum singular values, U_{Y_2} and V_{Y_2} are the matrices from the smallest singular value to the $N+1$-th maximum singular value. Thus, we transform the partial sum

minimisation of singular values into: $\arg\min_X \frac{1}{2}\|X-Y\|_F^2 + \tau\|X\|_{p=N}$, the above optimal solution can be solved by partial soft threshold operators:

$$\begin{aligned} D_{N,t}(Y) &= U_Y(S_{Y_1} + S_\tau[S_{Y_2}])V_Y^T \\ &= Y_1 + U_{Y_2}S_\tau[S_{Y_2}]V_{Y2}^T \end{aligned} \tag{10}$$

The entire algorithm flow is as follows:

Algorithm 1: IALM-based NIPPS solution

Input: original block image, weight factor $\hat{\lambda}$, singular value ratio γ

Output: background image B^k, Target image T^k.

initialization: $B^0 = T^0 = Y^0 = 0; \mu_0 = \frac{1.25}{\|D\|_2}; \mu_{\max} = 10^7; \rho = 1.5; \varepsilon = 10^{-7}; k = 0;$

1. First calculate N according to the given singular value ratio γ;

When the algorithm does not converge:

2. Fixed other parameter updates B, $B^{k+1} = D_{N,\mu_k^{-1}}(D - T^k + \mu_k^{-1}Y^k)$

3. Fixed other parameter updates T, $T^{k+1} = S_{\mu_k^{-1},\lambda\geq 0}(D - B^{k+1} + \mu_k^{-1}Y^k)$

4. Fixed other parameter updates Y, $y^{k+1} = Y^k + \mu_k(D - T^{k+1} - B^{k+1})$

5. Update μ, $\mu_{k+1} = \min(\rho\mu_k, \mu_{max})$

6. Check convergence conditions: $\frac{\|D - B^{k+1} - T^{k+1}\|_F}{\|D\|_F} < \varepsilon$

7. Update k, $k = k+1$

end

4. EXPERIMENTAL TEST

4.1 Experimental data

This paper tested the effectiveness of the algorithm model on 5 real data sets. Figure 3 shows several representative images, and Table 1 lists the detailed information. The selected image has large fluctuations, complex composition, and strong the edge of the background, the contrast of weak and small targets is poor, and the pixels are few. The selection of such images can better demonstrate the robustness of the proposed method .

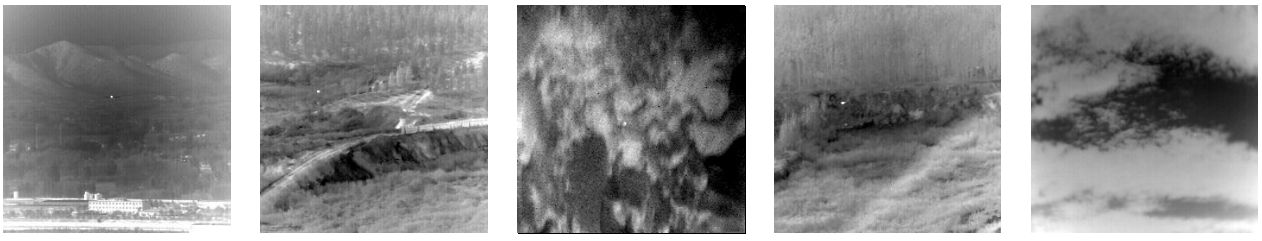

(a) (b) (c) (d) (e)

Figure 3. Five kinds of typical infrared data.

Table 1. Infrared image data information.

	Data amount	Data size	Target size	Background type
Data a	399	256×256	3×3	Mountains, trees, roads, houses
Data b	500	256×256	2×3	Ground, roads, trees
Data c	399	192×192	2×2	Complex cloud
Data d	178	256×256	2×4	The waves of the sea
Data e	399	320×240	2×1	Sky, clouds

4.2 Comparison method

To prove the availability of the algorithm proposed by us, the simulation results of this algorithm are compared with the classic infrared weak and small target detection methods such as LCM method. More advanced method such as RPCA method is compared. It mainly evaluates the capability of several detection methods from the result graph and quantitative indicators such as false alarm rate (FA), detection rate (PD), and SCR.

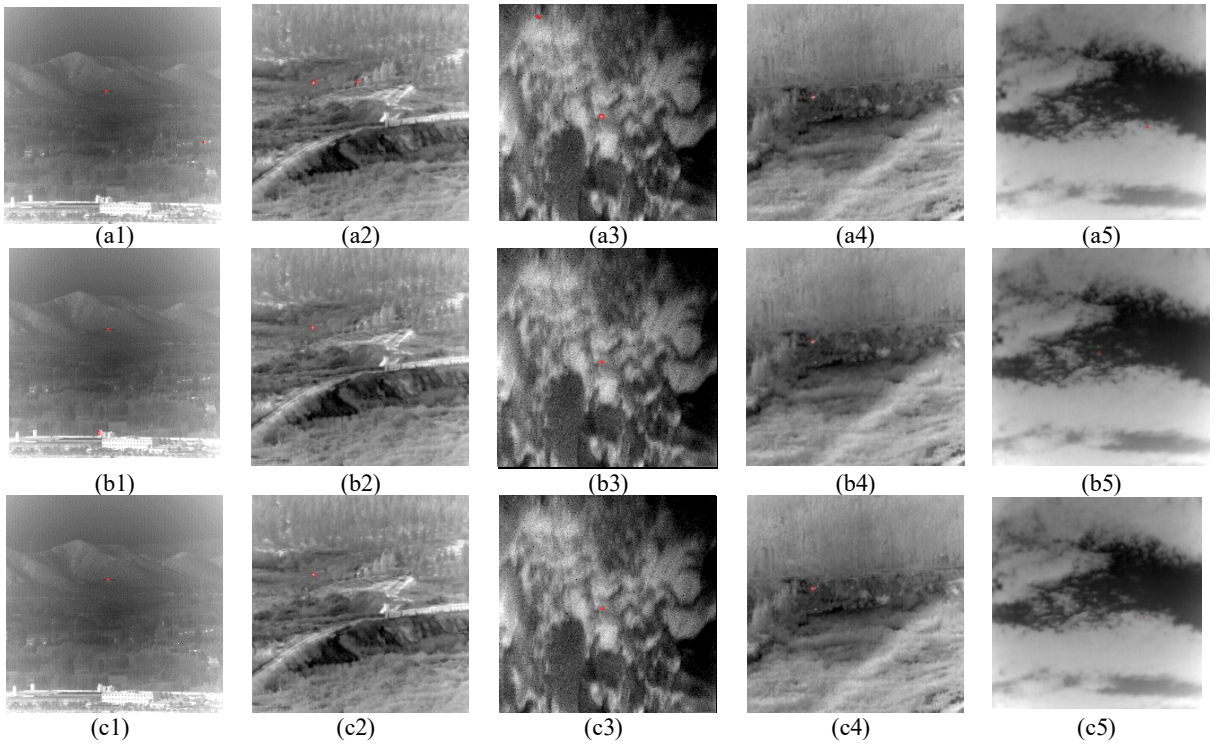

Figure 4. Diagram of the detection results of different methods. (a1)-(a5): detection results using LCM method; (b1)-(b5): detection results based on RPCA method; (c1)-(c5): detection results based on the proposed method .

Table 2. Detection results of various algorithms.

Detection algorithm	Detection accuracy (%)	False alarm rate (%)
LCM	84.4	21.6
RPCA	91.2	14.5
Our method	93.4	8.7

Detection rate and false alarm rate are important indicators of target detection. Table 2 shows the average results of infrared target detection in different scenarios and different clutter and noise conditions by 3 different algorithms. Table 2 shows that the algorithm proposed by us has better detection performance than other algorithms. The traditional detection method only uses a certain feature of the target to segment the target, which cannot be adapted to the complex and changeable situation. The method in this paper uses the method of multi-feature fusion to separate the candidate target and the background and detect it directly, a simple threshold method for effective target detection.

According to the subjective results in Table 4 and objective evaluation results in Table 2, it is shown that the algorithm proposed by us has high effectiveness in infrared image small target detection.

5. CONCLUSION

This paper proposes an infrared dim target detection on the ground of the partial combining Gaussian curvature and singular values. The infrared block image is obtained by preprocessing the infrared image by Gaussian curvature filtering. On the infrared block image, the RPCA method based on low-rank matrix and sparse matrix restoration is not effective in dealing with the edge effect, and the singular value part is used instead of the kernel norm. The method suppresses the background, and adopts a model solving algorithm based on the imprecise augmented Lagrangian multiplier method (IALM). The algorithm proposed in this paper can effectively deal with the clutter in the infrared image, and can be used for precise infrared guidance of remote small targets under complex background conditions. It is compared with other classic methods under different backgrounds, the results of simulation experiments verify the availability of the proposed algorithm.

REFERENCES

[1] Ye, X. and Xue, B., "Background suppression of infrared small target image based on inter-frame registration," Ninth International Conference on Graphic and Image Processing, (2018).

[2] Han, J., Yu, Y., Liang, K., et al., "Infrared small-target detection under complex background based on subblock-level ratio-difference joint local contrast measure," Optical Engineering, 57(10), 1(2018).

[3] Wan, M., Gu, G., Cao, E., et al., "In-frame and inter-frame information based infrared moving small target detection under complex cloud backgrounds," Infrared Physics & Technology, 76, 455-67(2016).

[4] Zhu, H., Liu, S., Deng, L., et al., "Infrared small target detection via low-rank tensor completion with top-hat regularization," IEEE Transactions on GeoScience and Remote Sensing, 58(2), 1004-1016(2020).

[5] Chen, C. L. P., Li, H., Wei, Y., et al., "A local contrast method for small infrared target detection," IEEE Transactions on Geoence & Remote Sensing, 52(1), 574-81(2013).

[6] Xia, C., Li, X., Zhao, L., et al., "infrared small target detection based on multiscale local contrast measure using local energy factor," IEEE Geoence and Remote Sensing Letters, (99), 1-5(2019).

[7] Qin, Y. and Li, B., "Effective infrared small target detection utilizing a novel local contrast method," IEEE GeoScience & Remote Sensing Letters, 1890-1894(2016).

[8] Liu, D., Cao, L., Li, Z., et al., "Infrared small target detection based on flux density and direction diversity in gradient vector field," IEEE Journal of Selected Topics in Applied Earth Observations and Remote Sensing, 1-27(2018).

[9] Wang X J, "Dim small target detection based on adaptive TDLMS algorithm," Electronics Optics & Control, 25(3), 78-80(2018).

[10] Xiong, B., Huang, X., Wang, M., et al., "Small target detection for infrared image based on optimal infrared patch-image model by solving modified adaptive RPCA problem," International Journal of Pattern Recognition and Artificial Intelligence, 35(02), (2020).

[11] Wang, C. and Qin, S., "Adaptive detection method of infrared small target based on target-background separation via robust principal component analysis," Infrared Physics & Technology, 69, 123-35(2015).

[12] Shi, Z., Wei, C. and Fu, P., "Small target detection in infrared image via sparse representation," Conference Record - IEEE Instrumentation and Measurement Technology Conference, 935-939(2015).

[13] Deng, L., Zhu, H., Zhou, Q., et al., "Adaptive top-hat filter based on quantum genetic algorithm for infrared small target detection," Multimedia Tools and Applications, 77(9), 10539-10551(2018).

[14] Li, H., Wang, Q., Wang, H., et al., "Infrared small target detection using tensor based least mean square," Computers & Electrical Engineering, 91, 106994(2021).

[15] Gao, C., Meng, D., Yang, Y., Wang, Y., Zhou, X., and Hauptmann, A. G., "Infrared patch-image model for small target detection in a single image," IEEE Transactions on Image Processing, 22(12), 4996-5009(2013).